

2D FLUID MODEL FOR INTERACTIVE DEVELOPMENT OF ICP TECHNOLOGICAL TOOLS

A.V. Gapon, A.N. Dahov, S.V. Dudin, A.V. Zykov, N.A. Azarenkov

V.N. Karazin Kharkov National University, 31 Kurchatov Ave., 61108, Kharkov, Ukraine,
e-mail: gapon@pht.univer.kharkov.ua

The software for ICP device simulation is worked out. Discharge chamber geometry, RF power, pressure and working gas type are the input data. The results of calculation are inductor voltage, ion current density distribution on the chamber surface, steady state space distributions of the electric field, plasma density and electron temperature in the chamber. Set of 2D parameter distributions is visualized immediately after calculation. The software had been carefully verified by comparing the calculation results with real data measured experimentally. The comparison has shown that both calculated 2D plasma density and electron temperature profiles and ion current density distribution on the processed surface are quite realistic. Graphical geometry input, fast calculation and immediate result visualization makes it possible to use our software for interactive development of ICP technological tools.

PACS: 52.35.Hr

1. BASIC EQUATIONS

In the paper [1] 2D fluid model was built which allowed to calculate basic parameters of ICP discharge in a simple cylindrical chamber. At the same time real technological ICP devices have chambers of more complicated shape. In this work we present software specifically aimed to solve this problem in arbitrary chamber of cylindrical symmetry. It calculates the electron density, electron temperature, electric field and particle flows distributions, if the chamber geometry, gas pressure and input power are given.

The problem is considered in cylindrical coordinates r, θ, z . The ambipolar diffusion and electron heat conductivity equations set was used for the transport processes modeling [2]:

$$-\nabla D_a \nabla n = N, \quad (1)$$

$$-\nabla \chi \nabla T = Q, \quad (2)$$

$$D_a = T / (m_i \nu_{ia}), \quad (3)$$

$$\chi = \frac{5}{2} \frac{nT}{m_e \nu_{ea}}, \quad (4)$$

$$N = \nu_i n, \quad (5)$$

$$Q = -3/2 \sum_j k_j + w \quad (6)$$

where n - plasma density, D_a - ambipolar diffusion coefficient, N - particle sources density, T - electron temperature, m_i, m_e - ion and electron masses, $\nu_i, \nu_{ea}, \nu_{ia}$ are the ionization, electron-neutral and ion-neutral collision frequencies, χ - electron heat conductivity, Q - heat sources density, p - working gas pressure, k_j - rate coefficient of j -th reaction between electron and neutral, w - input power density. We assume that particle velocity on the wall is equal to ion sound velocity $u_s = \sqrt{T/m_i}$.

Then, particle flow on the wall is:

$$-D_a \nabla n|_w = nu_s. \quad (7)$$

Heat flux on the walls is formed by the electrons with energies more than sheath potential drop. In the assumption of Maxwellian EEDF, the heat flux is:

$$-\chi \nabla T|_w = nT u_s \left(2 + \ln \sqrt{m_i/m_e} \right). \quad (8)$$

Expressions (7,8) make up the boundary conditions for (1,2). Rate coefficients were approximated from the data obtained with the help of BOLSIG+ program [3].

RF electric field \vec{E} with the angular frequency ω results in the electric current density \vec{j} in plasma, that in linear approach depends on \vec{E} by Ohm law:

$$\vec{j} = \sigma \vec{E}, \quad \sigma = i \frac{e^2 n}{m_e (\omega + i\nu_{ea})}, \quad (9)$$

where σ is the RF conductivity of plasma. Due to axial symmetry of the problem only angular component of the RF electric field is not equal to zero, $\vec{E} = (0, E_\theta, 0)$, therefore, it can't disturb the electric charge volume density ρ , because of plasma density does not depend on angle coordinate. Then $\nabla \cdot \vec{E} = 4\pi\rho = 0$, and from Maxwellian equations and quasi-static approach we obtain that

$$\Delta \vec{E} - \delta^{-2} \vec{E} = 0, \quad (10)$$

$$\delta^{-2} = -4\pi i \frac{\omega}{c^2} \sigma = \omega_p^2 / c^2, \quad (11)$$

where δ is the skin depth, ω_p is the plasma frequency.

Energy input in plasma is accounted as Joule heating and is described by term w in right part of (6):

$$w = \text{Re}(\vec{j} \vec{E}^*) / 2 = \frac{1}{8\pi} \frac{\omega_p^2 \nu_{ea}}{\omega^2 + \nu_{ea}^2} |E|^2 \quad (12)$$

Boundary conditions for (10) are

$$E_\theta = 0 \text{ on the metal walls} \quad (13)$$

$$[\nabla, \vec{E}]_{\tau_s} = i \frac{2\omega}{c^2 a} I \text{ on the inductor surface.} \quad (14)$$

In the (15) $\vec{\tau}$ is a unit vector tangential to the inductor surface and lied in (r, z) plane, a denotes wire radius of the inductor, and I - the amplitude of the electric current flowed through the inductor.

2. NUMERICAL SOLUTION

Transport equations set (1-2) and the equation for the electric field strength (10) are solved iteratively to obtain steady state self-consistent solution. The electric field, and then heat source density w do not vary when transport set is solved; in turn plasma density n , and then skin

depth δ are constant during the solution of the equation for electric field. An initial guess is needed the iterations to start. It is obtained from the eigenvalue problem solution ($T_e = const$ over the discharge chamber). Total power input in discharge is set to constant value and is one of the input parameters. Then, input power density w should be normalized correspondingly before the transport equations set is treated.

The code was totally realized in MATLAB-6.0.0.8 r12 environment because of excellent partial differential equation functions library (PDE toolbox) is included in it. In accordance with PDE toolbox paradigm, we should give the following form to the system of equations (1)-(6),(7)-(8):

$$-\sum_{j=1}^n \sum_{l=1}^2 \frac{\partial}{\partial x_k} C_{ijkl} \frac{\partial}{\partial x_l} u_j + A_{ij} u_j = F_i, \quad (15)$$

The boundary conditions of Neumann type looks as:

$$\sum_{j=1}^n \sum_{l=1}^2 \cos \alpha_k C_{ijkl} \frac{\partial}{\partial x_l} u_j + q_{ij} u_j = g_i. \quad (16)$$

In (15), (16) n is the number of equations, α_k is the angle between outward normal to the surface and direction of x_k axis. In the case of the transport equation set:

$$u = \begin{pmatrix} n \\ T \end{pmatrix}, \quad x = \begin{pmatrix} r \\ z \end{pmatrix}, \quad F = \begin{pmatrix} r \cdot N \\ r \cdot Q \end{pmatrix}, \quad (17)$$

$$C_{1111} = C_{1122} = r \cdot D_a, \quad (18)$$

$$C_{2211} = C_{2222} = r \cdot \chi, \quad (19)$$

$$q_{11} = u_s, \quad q_{22} = nu_s \left(2 + \ln \sqrt{m_i / m_e} \right). \quad (20)$$

For the electrostatics set (10, 13, 14) we have:

$$u = E_\theta, \quad C_{1111} = C_{1122} = -r, \quad A = -\omega_p^2 / c^2, \quad (21)$$

$$u|_{met} = 0, \quad g_1|_{ind} = i \frac{2\omega}{c^2 a} I, \quad (22)$$

where *met* and *ind* subscripts denote metal surfaces and inductor surface correspondingly. The value of inductor current I can be obtained during the normalization of w . All unmentioned components of C , A , q , g are equal to zero. After applying of finite element method transport equations take form

$$Ku = F, \quad (23)$$

where u is the solution vector and matrices K and F depend on u . We submit (23) in the traditional form for the nonlinear solvers applying:

$$Ku - F = A(u) = 0 \quad (24)$$

Equation (24) allows using the Newton iteration process in accordance with the known formula:

$$u^{n+1} = u^n + s \cdot (\partial A / \partial u \cdot u)^n, \quad (25)$$

where $\partial A / \partial u$ is the Jacoby matrix calculated on n -th iteration, s -parameter, which should be adjusted in limits $0.1 < s < 1$ for iteration convergence. All quantities included in A in (24) vary with u under calculation of $\partial A / \partial u$, with exception of w . The last is found in u^n and assumed to be constant under Jacoby matrix calculation.

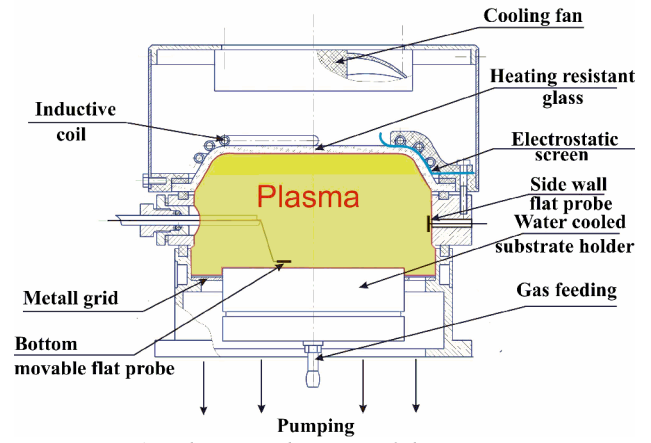


Fig. 1. Schematic diagram of the ICP reactor

3. COMPARISON WITH THE EXPERIMENT

The software had been verified by comparing the calculation results with real data measured experimentally.

Fig.1. presents sketch of the working chamber of the real setup used for the model testing and adjustment is shown. Inductive coil is fed by RF power of 0.1...1 kW range and 13.56 MHz frequency. Argon was used as working gas under pressures 0.3 mTorr...1 Torr. Fig.2 presents dependences of T and n on pressure.

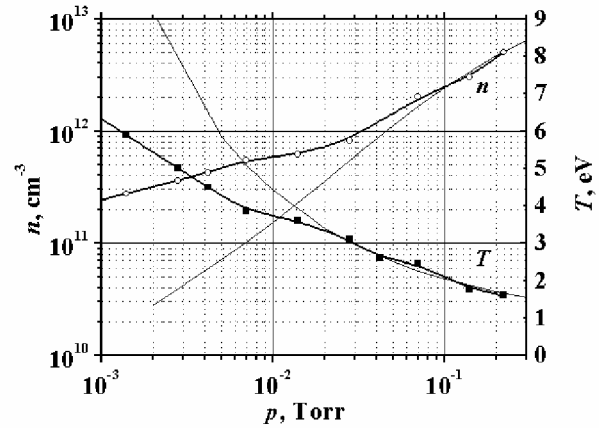


Fig.2. T and n in the chamber center vs. argon pressure. Bold lines – experimental results

Reliability of the model under low pressures (< 10 mTorr) is limited by the validity of the diffusive approach due to relatively high mean free path of charged particles. So, the discrepancies between measured and calculated values of T and n in the low pressure region looks natural.

Fig.3 depicts the radial dependence of the ion current density on the base of the chamber. The probe was set on the chamber axis. Calculated curves shows similar behavior with measured one. Presence of typical maximum ensures one in the model reliability.

Fig.4 shows normalized ion current density profiles on substrate holder.

At the Fig. 5 the set of calculated radial distributions of the ion current density on the substrate holder is presented. Sequence of profiles follows the behaviour of the curve on Fig. 2.

The comparison has shown that results of calculations at argon pressures > 0.01 Torr are in good agreement with all obtained experimental data.

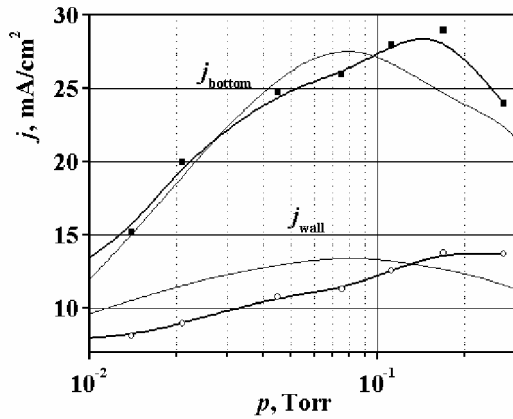


Fig.3. Ion current density at the chamber bottom and side walls vs. argon pressure. Bold lines – experiment

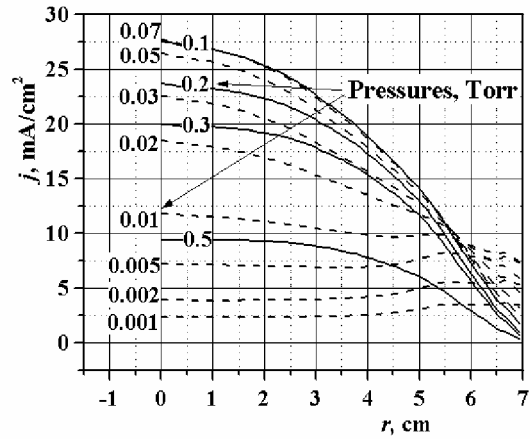


Fig.5. Pressure dependence of j radial profiles

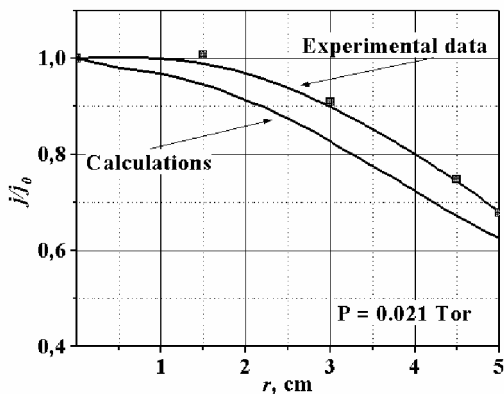


Fig.4 Normalized j profiles on the substrate holder

ACKNOWLEDGMENTS

This work was supported by Ministry of Industrial Policy of Ukraine, Project 92373/60

REFERENCES

1. I. Denysenko, S. Dudin, A. Zykov, N. Azarenkov. Ion flux uniformity in inductively coupled plasma sources//*Physics of Plasmas*. 2002, v.9, N11,p.4767-4775.
2. V.E. Golant, A.P. Zhilinskii and I.E.Sakharov. *Fundamentals of Plasma Physics*/ Moscow: "Atomizdat", 1977.
3. G.J.M. Hagelaar and L.C. Pitchford. Solving the Boltzmann equation to obtain electron transport coefficients and rate coefficients for fluid models//*Plasma Sources Sci. Technol.* 2005, v.14, p. 722–733.

ДВУМЕРНАЯ ГИДРОДИНАМИЧЕСКАЯ МОДЕЛЬ ДЛЯ ИНТЕРАКТИВНОЙ РАЗРАБОТКИ ТЕХНОЛОГИЧЕСКИХ УСТРОЙСТВ НА БАЗЕ ИНДУКТИВНОГО РАЗРЯДА

А.В. Гапон, А.Н. Дахов, С.В. Дудин, А.В. Зыков, Н.А. Азаренков

Разработано программное обеспечение для моделирования устройств, содержащих плазму индуктивного газового разряда. Входными данными являются геометрия камеры, вводимая мощность, давление рабочего газа. В результате расчёта получаются напряжение на индукторе, распределение тока ионов по поверхности разрядной камеры, установившиеся пространственные распределения электрического поля, плотности плазмы, и электронной температуры. Распределения искомых величин визуализируются непосредственно после вычисления. Результаты счёта тщательно сверялись с экспериментальными данными. Посчитанные распределения плотности и температуры плазмы, а также распределения ионного тока на обрабатываемой поверхности выглядят довольно реалистично. Графический интерфейс, скорость расчёта и непосредственная визуализация результата дают возможность использовать данное обеспечение для интерактивной разработки технологических установок.

ДВОВИМІРНА ГІДРОДИНАМІЧНА МОДЕЛЬ ДЛЯ ІНТЕРАКТИВНОЇ РОЗРОБКИ ТЕХНОЛОГІЧНИХ ПРИБОРІВ НА БАЗІ ІНДУКТИВНОГО РОЗРЯДУ

О.В. Гапон, О.М. Дахов, С.В. Дудін, О.В. Зыков, М.О. Азаренков

Розроблено програмне забезпечення для моделювання пристроїв, що містять плазму індуктивного газового розряду. Вхідними даними є геометрія камери, потужність, тиск робочого газу. Розрахунок дає напругу на індукторі, розподіл струму іонів на поверхні розрядної камери, просторові розподіли електричного поля, густини плазми, і електронної температури в камері. Розподіли шуканих величин відтворюються у графічному вигляді безпосередньо після обчислення. Результати обчислень ретельно порівнювалися з експериментальними даними. Розраховані розподіли густини та температури плазми, а також розподіли іонного струму на поверхні, що обробляється, виглядають досить реалістично. Графічний інтерфейс, швидкість розрахунку, та безпосередня візуалізація результату дають можливість використовувати дане забезпечення для інтерактивної розробки технологічного обладнання.